Absence of Compressible Edge Channel Rings in Quantum Antidots

I. Karakurt,[1] V. J. Goldman,[1] Jun Liu,[2] and A. Zaslavsky[2]

[1]*Department of Physics, State University of New York, Stony Brook, New York 11794-3800*

[2]*Department of Physics and Division of Engineering, Brown University, Providence, Rhode Island 02912*

(Received 6 December 2000; published 13 September 2001)

We report resonant tunneling experiments in a quantum antidot sample in the integer quantum Hall regime. In particular, we have measured the temperature T dependence of the peak value of a conductance peak on the $i = 2$ plateau, where there are two peaks per magnetic flux quantum ϕ_0. We observe a T^{-1} dependence as expected when tunneling through only one electron state is possible. This result is incompatible with tunneling through a compressible ring of several degenerate states. We also observe, for the first time, three conductance peaks per ϕ_0 on the $i = 3$ plateau.

DOI: 10.1103/PhysRevLett.87.146801 PACS numbers: 73.43.–f, 73.43.Jn, 73.63.–b

Resonant tunneling in *quantum* antidots (QAD) in quantum Hall (QH) regime provides a fascinating tool to study fundamental many body quantum mechanics. For example, a QAD electrometer has been used in the first direct observation of a fractionally quantized electric charge [1,2]. QAD is formed when a small potential hill is introduced into a two-dimensional electron system (2DES) subjected to magnetic field B (Fig. 1). First, neglecting electron-electron interaction and the antidot bare potential $U(r)$, in the symmetric gauge, single particle orbitals can be chosen to be eigenstates of the angular momentum with eigenvalues $\hbar m$, $m = 0, 1, 2, \ldots$. For an electron in the lowest Landau level these orbitals are

$$\psi_m(r, \theta) = (2\pi 2^m m!)^{-1/2} r^m \exp(im\theta - r^2/4), \quad (1)$$

where r is in units of magnetic length $\ell = \sqrt{\hbar/eB}$. All eigenenergies E_m in each spin-polarized Landau level are equal; that is, the states ψ_m are all degenerate. The peak value of $|\psi_m|^2$ occurs at $r_m = \sqrt{2m}\,\ell$, and the area within r_m is $S_m = 2\pi m\ell^2$; in other words, the WKB area of the orbital ψ_m encloses $m\phi_0$ of magnetic flux. Analogous QAD-bound basis wave functions can be written for each Landau level [3]. Insofar as $U(r)$ is weak, it can be treated perturbatively; the main effect is that the massive degeneracy of E_m is lifted.

In 2DES realized in GaAs/AlGaAs heterostructures, however, interelectron Coulomb interaction $\sim e^2/4\pi\epsilon\epsilon_0\ell$ is comparable to the cyclotron and Zeeman energies, and strongly mixes occupation of the basis orbitals, even between different Landau levels. Thus an appropriate theoretical description of a QAD has to be based on many electron wave functions, a goal not yet achieved. Because of lack of a rigorous theory two models have been advanced to describe tunneling experiments in samples with a QAD. One model postulates the existence of perfectly compressible rings of degenerate electron states circling the QAD, one ring per spin-split Landau level [4,5]. The observed discrete tunneling spectrum then requires lifting of degeneracy by Coulomb blockade, similar to lifting of degeneracy of electron states in metal particles [6].

We have used a different model [1,2,7]. Consider a 2DES region which includes the QAD, its boundary passing where chemical potential μ lies well within the QH gap, that is, where 2DES is "incompressible"; this region excludes any gapless edge channels connected to Ohmic contacts. Start with noninteracting electrons, Eq. (1), and gradually turn on interaction. Barring a phase transition

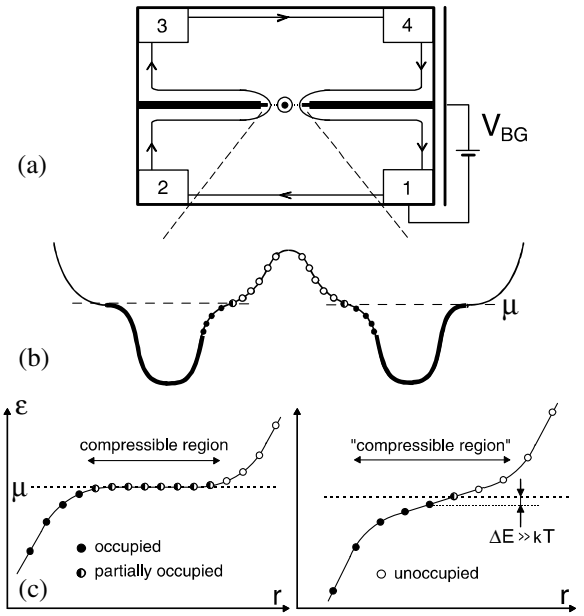

FIG. 1. (a) A quantum antidot sample. Numbered rectangles are Ohmic contacts; the antidot is in the constriction between two front gates. The arrowed lines show an edge channel. The back gate extends over the entire sample on the opposite side of the insulating GaAs substrate. (b) Self-consistent energy diagram of one Landau level in the constriction; the QHE gap forms the tunneling barriers. The energy spectrum is continuous at the edges and discrete near the antidot. (c) Two possibilities for the QAD-bound states near the chemical potential μ. The left version assumes a compressible ring of degenerate states; then the Coulomb blockade is required to lift the degeneracy. The right version illustrates that in a finite system perfect screening is not possible; then there is no truly compressible region at μ. At low T tunneling occurs between the left and the right edges via only one state.

[e.g., to a fractional quantum Hall (FQH) state] the states ε_m of the interacting 2DES are adiabatically connected to the states E_m of the noninteracting system. The eigenstates of the angular momentum are still eigenstates of the Hamiltonian, and we can use m to label them on each integer quantum Hall (IQH) plateau. Because perfect screening is impossible in a finite quantum system, the energy spectrum ε_m of the QAD region, including all interactions, is nondegenerate [8]. The ε_m depend on parameters, such as B and gate voltages, and on electron occupation. When B is varied, ε_m cross μ one by one. Small-bias single electron tunneling conductance peak occurs when $\varepsilon_m = \mu$ for the same m in the system without tunneling electron as well as in the system including the tunneling electron. We distinguish a continuous variable, filling factor $\nu = nh/eB$, and quantum number $i = h\sigma_{xy}/e^2$, where σ_{xy} is *quantized*. Because there are i electron states per ϕ_0 on the ith IQH plateau, the Aharonov-Bohm period $\Delta B = \phi_0/S$ contains i peaks, where S is the QAD area. When B is fixed, ε_m are affected by the electric field of the back gate at voltage V_{BG}; two consecutive conductance peaks are separated by ΔV_{BG} corresponding to the electric field required to attract one electron to area S [1,2].

In this paper we report resonant tunneling experiments in a QAD sample in the IQH regime. In particular, we have measured temperature T dependence of both the width W and the peak value G_p of a conductance peak on the $i = 2$ plateau. $G_p(T)$ is expected to be T independent when tunneling occurs through several degenerate states (a compressible ring), while the dependence is $G_p \propto 1/T$ for tunneling involving only one nondegenerate state. In the experiment we observe the $1/T$ dependence as T is varied by a factor of 10, which rules out lifting of the degeneracy by the Coulomb blockade.

We use low disorder GaAs heterojunction material, where 2DES ($n \approx 1 \times 10^{11}$ cm^{-2}, mobility 2×10^6 cm^2/V s) is prepared by exposure to red light at 4.2 K. The antidot-in-a-constriction geometry, somewhat different from that of [1,7], is defined by electron beam lithography on a preetched mesa with Ohmic contacts. After 150 nm of chemical etching, Au/Ti front gate metallization is deposited in the etched trenches. Samples are mounted on sapphire substrates with In metal which serves as the global back gate separated from 2DES by an insulating GaAs substrate 0.43 mm thick. The front gates are biased separately; the two voltages were adjusted to set the electron density (and therefore ν) in the constriction. Experiments were performed in a dilution refrigerator; extensive cold filtering cuts the electromagnetic background incident on the sample to 5×10^{-17} W, allowing us to achieve a low effective electron $T_{\mathrm{eff}} = 18$ mK [9].

Figure 2 shows the four-terminal magnetoresistance R_{xx} in the IQH regime. We use ν_{C} as the filling factor in the constriction region between the front gates, and ν_{B} for "the bulk," away from the constriction region. The front gates are biased negatively to bring the edges closer to the antidot to increase the tunneling amplitude

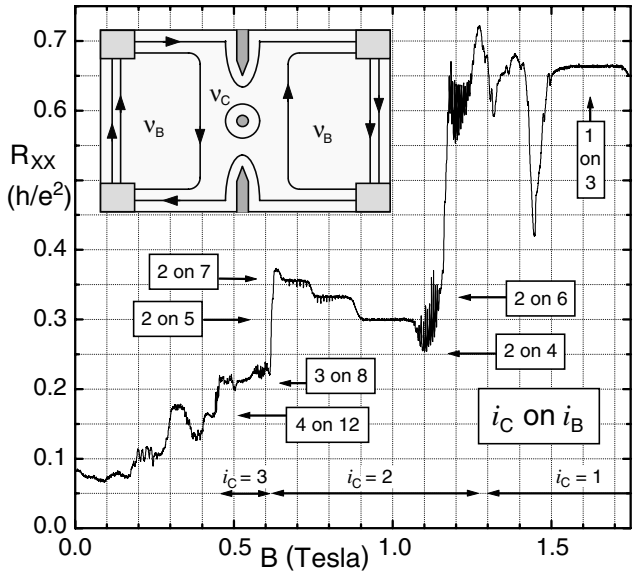

FIG. 2. Four-terminal R_{xx} vs B in the integer QH regime; horizontal arrows (labeled i_{C} on i_{B}) show quantized values of R_L. The negative bias on the front gates depletes the antidot-constriction region so that ν_{C} is smaller than ν_{B} in the bulk. The inset illustrates the case $\nu_{\mathrm{C}} \approx 1$ on $\nu_{\mathrm{B}} \approx 2$.

to a measurable level; this results in ν_{C} being smaller than ν_{B}. A quantum Hall effect (QHE) sample with two ν_{B} regions separated by a lower ν_{C} region has $R_{xx} = R_L \approx R_{xy}(\nu_{\mathrm{C}}) - R_{xy}(\nu_{\mathrm{B}})$, if no tunneling occurs. The equality is exact, $R_L = (h/e^2)(1/i_{\mathrm{C}} - 1/i_{\mathrm{B}})$, if both filling factors are on a plateau, $\nu_{\mathrm{C}} \approx i_{\mathrm{C}}$ and $\nu_{\mathrm{B}} \approx i_{\mathrm{B}}$, which can be achieved by adjusting the front gate voltages. Then the Hall resistances R_{xy} of all regions acquire quantized values. Several R_L plateaus (neglecting tunneling peaks) are seen in Fig. 2.

Resonant tunneling through QAD results in characteristic R_{xx} peaks quasiperiodic in B. In some data we observe both R_{xx} peaks for $\nu_{\mathrm{C}} < i_{\mathrm{C}}$, "back scattering," and dips for $\nu_{\mathrm{C}} > i_{\mathrm{C}}$, "forward scattering" [4,10]; see the $i_{\mathrm{C}} \approx 2$ plateau in Fig. 2. The tunneling peaks are superimposed on a smooth R_L background, and we obtain tunneling conductance G_T as described previously [1,9]. In essence, when R_L is quantized, edge network model gives $G_T = (R_{xx} - R_L)/[R_H^2 - R_H(R_{xx} - R_L)]$, where constriction Hall resistance $R_H = h/i_{\mathrm{C}}e^2$. Both back ($R_{xx}$ peaks) and forward (R_{xx} dips) scattering results in G_T peaks. Thus determined G_T vs B data for R_{xx} peaks on $i_{\mathrm{C}} = 1$, 2, and 3 plateaus are shown in Fig. 3. As expected, there are i_{C} peaks per $\Delta B \approx 11.5$ mT, corresponding to the addition of one ϕ_0 to the QAD area S_μ at the chemical potential μ; thus S_μ is approximately the same for all the plateaus. Note that $\phi_0/2$ and $\phi_0/3$ periodicities follow naturally from our i peaks per ΔB model, and do not require invocation of Coulomb blockade. From ΔB we immediately obtain the antidot radius $r_\mu = \sqrt{\phi_0/\pi\Delta B} \approx 340$ nm; the quantum number $m_\mu = B/\Delta B \approx 75, 80$, and 190 for the $i_{\mathrm{C}} = 3, 2$, and 1 plateaus, respectively.

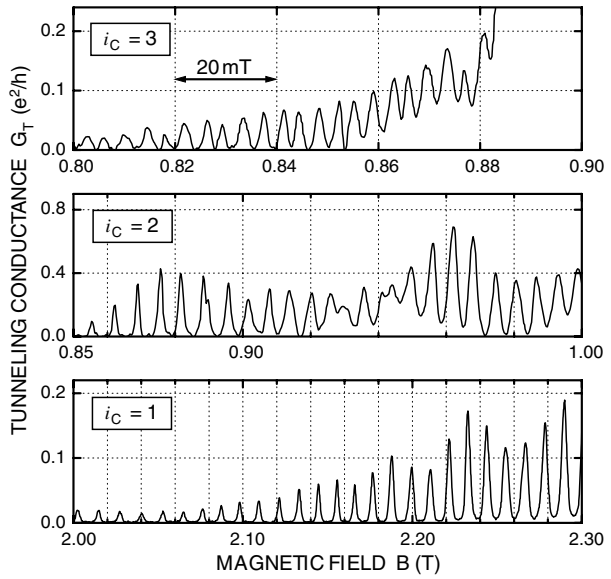

FIG. 3. Representative G_T vs B data for $i_C = 1, 2,$ and 3 plateaus. B is scaled as 1:2:3, and the vertical grid lines are spaced by 20 mT in all three panels.

The small-bias tunneling conductance has been calculated for an on-site interaction model appropriate to our experiments [11,12]. For the classical Coulomb blockade regime $\Gamma, \Delta\varepsilon \ll k_B T$, when tunneling occurs through many degenerate states [6,13],

$$G_T = G_p \frac{(\mu - \varepsilon_0)/k_B T}{\sinh[(\mu - \varepsilon_0)/k_B T]}, \quad G_p = \frac{e^2}{h} \frac{\rho \Gamma_L \Gamma_R}{2\Gamma}, \quad (2)$$

where Γ_L and Γ_R are the tunneling rates to the right and the left leads, $\Gamma = (\Gamma_L + \Gamma_R)/2$, ε_0 is the energy of the resonant state, and ρ is the density of states at the chemical potential μ. For $\Gamma, k_B T \ll \Delta\varepsilon$, when only one nondegenerate electron state is involved in resonant tunneling, conductance is given by [9,14]

$$G_T = \frac{e^2}{h} \frac{\Gamma_L \Gamma_R}{4 k_B T} \int d\varepsilon \, \frac{1}{(\varepsilon - \varepsilon_0)^2 + \Gamma^2} \cosh^{-2}\left(\frac{\mu - \varepsilon}{2 k_B T}\right), \quad (3)$$

If $k_B T \gg \Gamma$, thermal broadening dominates, and Eq. (3) becomes

$$G_T = G_p \cosh^{-2}\left(\frac{\mu - \varepsilon_0}{2 k_B T}\right), \quad G_p = \frac{e^2}{h} \frac{\pi \Gamma_L \Gamma_R}{4 k_B T \Gamma}. \quad (4)$$

When lifetime broadening dominates, $\Gamma \gg k_B T$, the conductance peak takes a Lorentzian form:

$$G_T = (e^2/h) \Gamma_L \Gamma_R [(\mu - \varepsilon_0)^2 + \Gamma^2]^{-1}. \quad (5)$$

The R_{xx} dips on the low-B side of the $i_C = 2$ plateau in Fig. 2 have $\Delta B \approx 18$ mT; here $r_\mu \approx 270$ nm. Figure 4(a) shows the corresponding conductance G_T as a function of V_{BG}. The peaks are well separated at low bath $T = 11.8$ mK; we therefore studied the line shape and the T dependence of these G_T vs V_{BG} peaks in detail. A high-resolution sweep of the peak at $V_{BG} = -1.3$ V is plotted in Fig. 4(b) with two line shape fits. We compare experimental G_T to Eqs. (2)–(5) to see whether it is possible to ascertain that the experiment is in one of the various regimes. In experiment G_T is measured as a function of B or a gate voltage (in our case V_{BG}), at several T; as before [8,9], we can relate experimental parameters to the energy tuning via linear terms of expansions: $\mu - \varepsilon_0 = \beta(B_0 - B) = \alpha(V_{BG} - V_{BG0})$. Since α, β, Γ_L, and Γ_R are not known independently in practice, the only rigorous analysis possible is to compare normalized line shapes G_T/G_p vs V_{BG} or B, and experimental T dependencies $G_p(T)$ and $W(T)$ to Eqs. (2)–(5). Here W is the appropriate "width" parameter of the normalized line shapes G_T/G_p vs V_{BG}. The solid line is the best fit to thermally broadened line shape Eq. (4), which becomes $G_T = G_p \cosh^{-2}[(V_{BG0} - V_{BG})/W]$ using experimental observables. The fitting parameters are the peak amplitude G_p, the width W, and the peak position V_{BG0}. The dashed line is the best fit to Eq. (5); it does not give a good fit even at the lowest T, ruling out the intrinsic linewidth regime $\Gamma \gg k_B T$. The thermally broadened line shape Eq. (4) fits our data very well at all experimental T. It so happens that the functional dependence $x/\sinh x$ in Eq. (2) is very close to $1/\cosh^2(\sqrt{6}\,x)$ in Eq. (4) for $x < 8$. The *absolute* energy scale is different by a factor of $\sqrt{3/2}$; however, it can be determined only from the T dependence of W [8], which requires the use of one of the models. Thus, even though the line shapes of Eqs. (2) and (4) are not identical, both fit the data equally well.

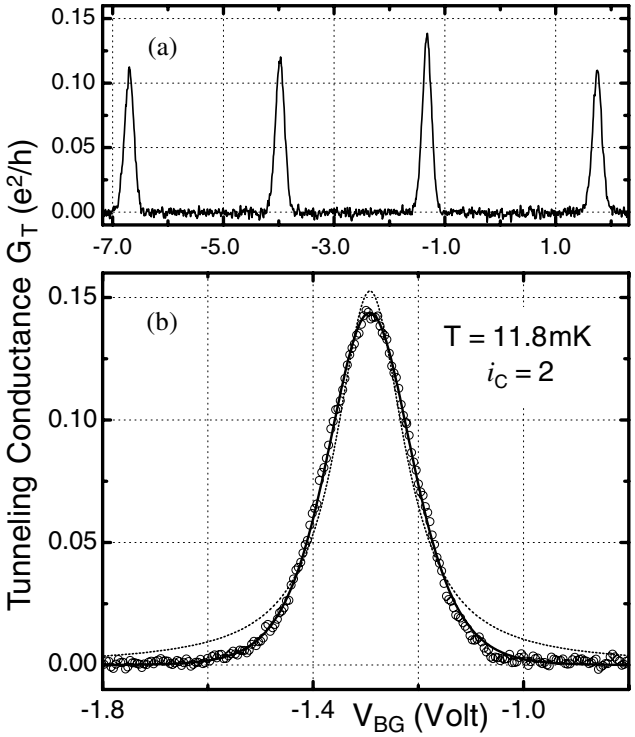

FIG. 4. (a) G_T vs V_{BG} for R_{xx} dips on the low-B side of the $i_C = 2$ plateau at $B = 0.804$ T. (b) High-resolution sweep data (circles) of one of the peaks. Solid line is the best fit to Eq. (4). Dotted line is the best fit to a Lorentzian Eq. (5).

In Fig. 5 we plot G_p and the width W as a function of T, obtained from fits of the experimental G_T vs V_{BG} peak of Fig. 4(b). The solid lines are two-parameter phenomenological fits: $W = (2k_{\mathrm{B}}/\alpha)\sqrt{T^2 + T_0^2}$ and $G_p = G_{p0}/\sqrt{T^2 + T_0^2}$, where α, G_{p0}, and T_0 were varied for the best fit [15]. The width W increases monotonically with T, and the dependence is linear at high temperatures. The peak value G_p decreases monotonically with increasing T, and $G_p \propto 1/T$ dependence is clear for $35 < T < 320$ mK, consistent with Eq. (4), derived for resonant tunneling through one nondegenerate state. The dashed line gives $G_p(T) = G_{p0}$, which is the prediction of Eq. (2) derived for tunneling through many degenerate states, when only Coulomb blockade lifts degeneracy. The constancy of $G_p(T)$ for tunneling through several degenerate states, $\Delta\varepsilon \ll k_{\mathrm{B}}T$, when only Coulomb blockade produces conductance peaks, is quite fundamental: it results from the $\propto 1/T$ dependence of tunneling through each state being canceled by the $\propto T$ increase in the number of states participating in tunneling. In fact, in this regime $G_p(T)$ even increases at higher T [12]. Thus, the data of Fig. 5 rules out that tunneling occurs via a degenerate "compressible ring" of QAD-bound electron states in our samples.

From Eq. (4) $\alpha W = 2k_{\mathrm{B}}T$; the fit gives $\alpha = 56.5\ \mu\mathrm{eV/V}$. We can obtain "addition energy" level spacing $\alpha\Delta V_{\mathrm{BG}} \approx 150\ \mu$eV from the activation energy at a minimum between two consecutive tunneling peaks [16]. This is a sizable fraction of the cyclotron energy (1.4 meV), and is greater than the bare Zeeman energy (17 μeV). Both α and $\Delta\varepsilon$ in the present sample are greater by a factor of 5 than in the sample of Refs. [1,8], even though the lithographic size of the antidot is nearly the same, and the QAD area S obtained from the Aharonov-Bohm period is 30% greater in the present sample. The largest possible variable is the etching depth, which is not known very accurately. The etching depth strongly affects the bare antidot potential $U(r)$, which is due to GaAs surface depletion in our samples. This is additional evidence that the self-consistent electrostatics of *interacting* electrons is responsible for the energetics in a QAD.

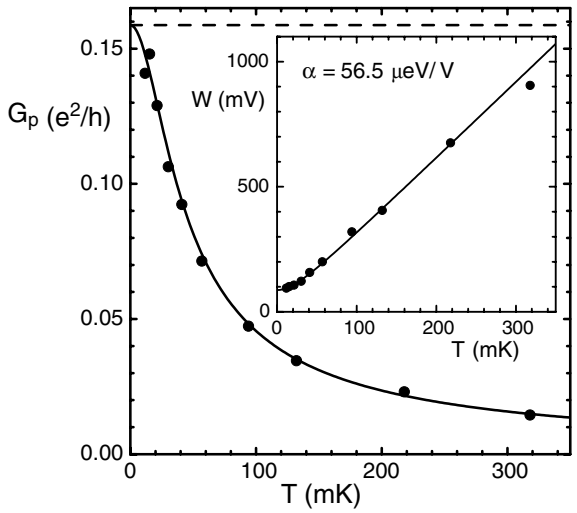

FIG. 5. Peak tunneling conductance G_p vs temperature T. For $35 < T < 320$ mK, $G_p \propto 1/T$ (solid line), as expected for resonant tunneling through only one nondegenerate state. The dashed line gives the expectation for tunneling through a ring of degenerate states, with Coulomb blockade lifting degeneracy. Inset shows the dependence of the width parameter W; for $T > 35$ mK, $W \propto T$ (solid line).

In summary, we have measured the T dependence of both the width and the peak value G_p of a conductance peak on the $i = 2$ IQH plateau. The observed $G_p \propto 1/T$ dependence is consistent with resonant tunneling through only one nondegenerate QAD-bound state, and rules out the regime of tunneling through several degenerate states (a compressible edge channel ring), when G_p is expected to be T independent. We also observed, for the first time, three conductance peaks per ϕ_0 on the $i = 3$ plateau.

This work was supported in part by the NSF under Grant No. DMR9986688. The work at Brown was supported by an NSF Grant No. DMR9702725 and the NSF MRSEC Center Grant No. DMR9632524.

[1] V. J. Goldman and B. Su, Science **267**, 1010 (1995).
[2] V. J. Goldman, Physica (Amsterdam) **1E**, 15 (1997).
[3] *The Quantum Hall Effect,* edited by R. E. Prange and S. M. Girvin (Springer, New York, 1990), 2nd ed.; S. M. Girvin, *The Quantum Hall Effect,* Les Houches Lecture Notes (Springer-Verlag, New York, 1998).
[4] C. J. B. Ford *et al.,* Phys. Rev. B **49**, 17 456 (1994).
[5] M. Kataoka *et al.,* Phys. Rev. B **62**, R4817 (2000); Phys. Rev. Lett. **83**, 160 (1999).
[6] D. V. Averin and K. K. Likharev, in *Mesoscopic Phenomena in Solids* (Elsevier, Amsterdam, 1991).
[7] Aside from accidental degeneracy.
[8] I. J. Maasilta and V. J. Goldman, Phys. Rev. B **57**, R4273 (1998).
[9] I. J. Maasilta and V. J. Goldman, Phys. Rev. B **55**, 4081 (1997).
[10] J. K. Jain and S. A. Kivelson, Phys. Rev. Lett. **60**, 1542 (1988).
[11] Y. Meir, N. S. Wingreen, and P. A. Lee, Phys. Rev. Lett. **66**, 3048 (1991).
[12] C. W. J. Beenakker, Phys. Rev. B **44**, 1646 (1991).
[13] L. I. Glazman and R. I. Shekhter, J. Phys. Condens. Matter **1**, 5811 (1989).
[14] Similar analysis for a few-electron quantum dot was reported in B. Su, V. J. Goldman, and J. E. Cunningham, Science **255**, 313 (1992); Phys. Rev. B **46**, 7644 (1992).
[15] In this experimental run the filtering was reduced for the IQH effect regime, and the lowest effective electron temperature $T_0 \approx 27$ mK is higher than 18 mK obtained in the FQH effect regime [8,9].
[16] We note that the T dependence of G_T at the minima between peaks depends on the peak separation, and thus is not universal. Therefore an analysis that involves *amplitude* of conductance oscillations, such as Fourier transform of the conductance data, is, in general, ambiguous.